

Surfzone wave characteristics during floodtide on the central west coast of India

Jaya Kumar Seelam

CSIR-National Institute of Oceanography, Dona Paula, Goa 403 004, INDIA
Academy of Scientific and Innovative Research, School of Oceanography, Goa, INDIA
email: jay@nio.org; Tel: +91-832-2450316 [Corresponding Author]

Jishad, M

Academy of Scientific and Innovative Research, School of Oceanography, Goa, INDIA
CSIR-National Institute of Oceanography, Dona Paula, Goa 403 004, INDIA
email: jishadm@nio.org

Yadhunath, E. M

CSIR-National Institute of Oceanography, Dona Paula, Goa 403 004, INDIA
email: yadhunathm@nio.org

Rajasekaran, C

CSIR-National Institute of Oceanography, Dona Paula, Goa 403 004, INDIA
email: rajasekaranc@nio.org

Gowthaman, R

CSIR-National Institute of Oceanography, Dona Paula, Goa 403 004, INDIA
email: rgowtham@nio.org

Pednekar, P. S

CSIR-National Institute of Oceanography, Dona Paula, Goa 403 004, INDIA
email: pprem@nio.org

Ryan Luis

CSIR-National Institute of Oceanography, Dona Paula, Goa 403 004, INDIA
email: rluis@nio.org

PrakashMehra

CSIR-National Institute of Oceanography, Dona Paula, Goa 403 004, INDIA
email: pmehra@nio.org

Abstract

Surfzone wave characteristics, measured using a wave and tide gauge during a flood tide, were studied at three different beaches having different nearshore slopes. The spectral wave characteristics viz., wave height and mean wave period were estimated considering different sample sizes. Inter-comparisons of wave climate between each of three beaches for a similar tide level are presented. The wave height and mean wave period values obtained from the wave analysis for each of the record using waves by wave method show that surfzone wave height increased with time during a flood tide and the mean wave period decreased with time up to mid tide and then increased during the rest of the measurement period at Keri and Miramar beaches. At Candolim, the reversing trend of mean wave period increase is observed to occur much before reaching the mid tide level. The surf zone waves during a flood tide indicated that the wave heights increased with time while the mean wave period showed a decreasing trend in general. The variation of breaker index showed a decreasing trend from low tide to high tide ranging between 0.45 and 0.23. The surf similarity parameter estimated corroborates with the visual observations.

Key words: surfzone, long period waves, breaker index, tide modulation, spectra

1. Introduction

Ocean waves are of fundamental interest for many aspects including engineering design and operation in coastal and offshore industries. Study of wave characteristics has a great importance in sediment transport and coastal processes which helps in the study of coastal erosion. Beach erosion is an universal problem and it has been estimated that 70% of all the beaches in the world are eroding (Bird, 1985). Waves dissipate their energy through breaking in the surfzone and the surf zone wave climate is the net outcome of the wave refraction, reflection, diffraction and wave breaking, combined with nearshore waves, currents and sediment interaction (e.g., Dean and Dalrymple, 2010; Nielsen, 2009). Surfzone waves are one of the major factors influencing the beach morphology, beach characteristics and planning and designing of a coastal protective structures (e.g., Hamm et al., 1993). Study of surfzone wave characteristics has great importance in the study of nearshore sediment transport and coastal morphology processes.

The surfzone hydrodynamics were studied across the globe by many researchers (e.g., Apotsos et al., 2008; Basco, 1983; Dally et al., 1985; Madsen et al., 1997; Power et al., 2010; Sørensen et al., 1998; Thornton and Guza, 1986) and is still an active subject of research. Most of the

studies pertain to the laboratory investigations on various aspects like longwave generation in the surfzone due to release of bound waves from wave breaking (e.g., Baldock, 2006; Baldock et al., 2004; Baldock and Huntley, 2002; Baldock et al., 2000; Dong et al., 2009; e.g., Guza et al., 1984; Janssen et al., 2003; Longuet-Higgins and Stewart, 1962; Munk, 1949; Tucker, 1950); surfzone and swashzone sediment transport (e.g., Chandramohan et al., 1993; Elfrink and Baldock, 2002; Fredsøe and Deigaard, 1992; Omran et al., 2010; Reginald and Richard, 1988; Rogers and Ravens, 2008; Sanil Kumar et al., 2003; Sanil Kumar et al., 2004); etc. There are not many studies that are based on direct instrumented measurements in the surfzone in water depths less than 3 m and especially the variation of surfzone waves during a flood tide in coastal waters of India. Earlier studies by Thornton & Guza(1986) as well as Apotsos et al(2008) looked at the variation of surfzone wave height variation and wave setup in the surfzone but did not discuss on the wave height variation with tide. This study considers the variation of wave heights under the tidal influence as well as presents a new set of data on surfzone waves and its dynamics in a micro to meso-tidal regime on the central west coast of India.

2. Study Region

The geographic positions of three beaches in Goa (Fig. 1), where the study is carried out, are given in Table 1. The Wave and Tide Gauge (WTG) was deployed on three different dates at the following positions respectively for Miramar beach (Latitude 15°28'49.26"N; Longitude 73°48'20.08"E) (Fig. 2), Candolim beach (Latitude 15°30'31.78" N; Longitude 73°45'53.56"E) (Fig. 3) and Keri beach (Latitude 15°42'56.44" N; Longitude 73°41'25.09"E) (Fig. 4). These three beaches were considered as each of these beaches has a different coastal profile, foreshore slope and the surfzone conditions are quite different. Miramar beach lies adjacent to the confluence of River Mandovi with the Arabian Sea, is a crescent shaped beach within the 3 km region between the Cabo headland in the south and Aguada headland in the north. The northern region of Miramar beach is oriented almost N-S and is influenced by the interaction of waves with the navigation channel and the river flow as well. The beach south of the river confluence is a low energy beach as the surfzone width is comparatively large as the waves break over a longer distance and dissipate much of their energy before reaching the shore. The waves at Miramar beach are mostly of surging breakers. Candolim beach is a region within a longer stretch of beach about 7.5 km between Aguada headland and Baga headland. Candolim beach was heavily influenced by a grounded ship, about 500 m from shore, which acted as an offshore breakwater, resulting in formation of a salient and further influencing the surrounding surfzone. The superstructure of the grounded ship (shown as shaded region in Fig. 3) has been recently removed allowing the waves to traverse the hitherto obstructed

region. However, recent underwater survey showed the vessel hull buried below the bed, which would act as non-eroding bed and thus would influence the coastal morphology and the surfzone around it. The waves at Candolim are of plunging and spilling type. Keri beach is a 1.5 km long beach with the River Terekol having its confluence with Arabian Sea in the northern part of Keri beach and a headland is present on the southern part. Keri beach is almost a straight beach oriented 345° with respect to North and has a dynamic sand spit in the confluence region which disappears during the southwest monsoon and reappears during the calm seasons. Keri beach experienced erosion during the past decade and hence a protective wall was constructed all along the beach. The middle portion of Keri beach was severely eroded few years ago and is again protected recently with tetrapods on the high tide line. The nearshore region of Keri beach, where the wave measurements were carried out, is steep and the coast is observed to be reflective. The waves are of plunging type with occasional spilling breakers. The foreshore beach slopes of Miramar, Candolim and Keri are 0.0273, 0.08 and 0.12 respectively.

3. Methodology

The Seabird[®] SBE 26 SEGAUGE Wave and Tide recorder (WTG) is self-contained in a rugged non-corroding plastic housing with a standard Quartzonix pressure sensor with a 20 meter water depth rating and a temperature-compensated quartz element. The WTG is fixed inside a protective casing and was deployed in water depth less than 1 m during low tide period. Tide measurements are obtained by continuously counting the pressure frequency with a 40-bit ripple counter that resets after every set of recording. The real-time clock is continuously powered has an accuracy of 5 ppm and a resolution of 2 milliseconds. The Wave burst measurements are made with a period counter, with its time base generated from a temperature-compensated, precision quartz crystal oscillator. The tide resolution is 0.2 mm for 1 minute averaged data and the wave resolution is 0.4 mm for 4 Hz integration. The accuracy of the pressure sensor is 0.01% full range (= 0.3mm for 20 m pressure rating) (Anonymous, 2011). In the present study, the tide measurement is averaged over 2 minutes at 20 minutes interval and the waves are measured continuously for 17 minutes at a sampling interval of 4 Hz. The same WTG was deployed separately at the three beaches during three consecutive days around low tide time and retrieved around the high tide time.

The measured time series wave data at each of the beach were retrieved from the WTG using Seabird proprietary software and the raw data is used for further analysis. The measurements were planned for a period of 140 min so as to obtain 7 records of 20 minutes each for all the three beaches. The measurement period spanned over more than half of the tide duration between low tide and high tide,

covering most of the flood tide period. The deployment of WTG was carried out close to the low tide time due to which the low tide wave measurements were not recorded. However, the first set of measurements were closer to the low tide time and so the first wave record set measured immediately after deployment of WTG is referred further as low tide data. The wave record measured before retrieval of the WTG is referred as high tide data (at Candolim this represent mid tide period) and the measured data midway through the measurement period is referred as mid tide period. At Candolim, the WTG started to get buried under the sand after recording 5 data sets and therefore WTG was retrieved; hence the last 2 data sets were not recorded at Candolim.

Each wave record consisted of 4096 data points measured over a period of 17 minutes each. The wave record is firstly passed through a Butterworth filter with cut-off frequencies being 0.3 and 2 Hz to smoothen the raw data. Two schemes were adopted to obtain wave spectra using Fast Fourier Transformation analysis (FFT). FFT analysis requires 2^n number of data points, where n is the integer having value of 1, 2, 3, etc. up to infinity. In the first scheme the wave record with 2048 ($=2^{11}$) data points corresponding to 256s was used to obtain a single wave spectrum. In the second scheme wave record of 256 ($=2^8$) data points corresponding to 32 s was used to obtain a spectra. Further 8 such spectra were obtained from adjoining wave records of 256 points each (total wave record of 256s) and all these 8 spectra were averaged to obtain an averaged spectrum. The second scheme is used in analysis of wave records in Waverider buoys (Kuik et al., 1988). All of the data in each of the wave record is used in FFT analysis. The various wave parameters viz., significant wave height (H_s), maximum wave height (H_{max}), mean wave height (H_{mean}), average of maximum 10% waves ($H_{1/10}$), wave period corresponding to peak spectral wave energy and mean wave period are obtained from the wave analysis tool box from WAFO (WAFO, 2000). The Iribarren number also known as surf similarity parameter was calculated for all the three beaches, $\xi = \tan \beta / \sqrt{(H_b / L_0)}$, where H_b is the breaker wave height, L_0 is offshore wave length. This is carried out to ascertain the type of breakers associated with the beach slope and its variation with time. The beach slopes were taken from the measurements on the beach profiles (Seelam et al., 2014). The beach slopes at Miramar, Candolim and Keri were 0.026, 0.066 and 0.14 respectively.

4. Results And Discussion

Measurements on the surfzone waves carried out at the three beaches are analysed to study their dynamics during a flood tide. The location of WTG deployments in the surfzone over the measured cross-section profile at Miramar, Candolim and Keri are shown in Figs 2, 3 and 4 respectively. The zero elevation in Figs. 2 to 4 represents the elevation of temporary benchmark with

respect to which the beach profile monitoring is regularly carried out by the authors. In this study, the wave data collected by the WTG over a flood tide period on spring tidal days is considered. The data analysis is carried out for all the wave records measured at 20 minutes interval over a period of 1 hour 40 minutes at Candolim and 2 hours 20 minutes for Miramar and Keri. However, only the low, mid and high tide wave records for each of the beach are discussed here so as to arrive at the variations in surfzone wave climate over a flood tide. The water level variations during the three different observation periods are presented in Fig. 5 along with the predicted tide for Mormugao Port.

The wave height variation with time for Miramar beach during low tide (wave record immediately after deployment), mid tide (i.e., midway through the measurement) and near high tide (i.e., before retrieval of the equipment) respectively is presented in Fig. 6(a) to 6(c); for Candolim corresponding wave height variations are shown in Figs. 7(a) to 7(c) and for Keri in Figs. 8(a) to 8(c). A record length of 2048 points was considered for the analysis. During low tide, a superimposed long wave is clearly observed, whereas during the high tide wave group envelope is obvious, except for Keri during high tide. Moreover, the wave height range, in general, appeared to increase with increasing tide for all the three locations. In order to clearly arrive at these apparent observations from the smoothed raw data were further subjected to standard FFT technique to obtain the wave characteristics for each wave record. Further averaging of the wave data is not carried out to show the wave form variation as well. Detailed analysis of long waves and wave groups is not addressed in this paper. During high tide the wave amplitude range at Miramar was between -0.2 and 0.25m, whereas during low tide the amplitude range was between -0.1 and 0.1m (Fig. 6). At Candolim beach during the low tide the wave amplitude was between -0.1 and 0.2m and during high tide it was between -0.2 and 0.3m (Fig. 7). The wave amplitude range for Keri beach during low tide was between -0.1 and 0.1m and during high tide it was between -0.12 and 0.25 m (Fig. 8).

Waves on Miramar and Candolim beaches showed similar wave forms during all the different tides. During low tide, the wave form was like a bore with short crest and a long trough (Fig. 6(a) and Fig. 7(a)), due to the longer dissipating zone. However, on Keri beach, during the low tide, the wave form did not show a conspicuous bore like form, as the surfzone width was very short, owing to steeper nearshore slope, and with waves breaking close to the waterline (Fig. 8(a)). During mid-tide, both at Miramar and Candolim beaches the waves were found to show variable wave forms, at times similar to that of low tide and for the rest of the time similar to that of high tide (Figs. 6(b) and 7(b)).

Each surface elevation record ($\zeta(t)$) was subjected to Fast Fourier Transformation (FFT) and the wave spectrum was obtained. The wave spectrum for the wave record immediately after deployment (referred as low tide period), in between the deployment midway through the measurement (referred as mid tide period) and before retrieval of the equipment (referred as high tide periods) at Miramar, Candolim and Keri are presented with frequency (Hz or s^{-1}) on the abscissa and spectral amplitude (FFT (ζ)) denoted as $|Y(f)|$ in m^2/Hz on the ordinate. The frequency axis is plotted only up to 0.5Hz (2 s) as higher frequency values are in general irrelevant in the gravity water wave studies. Two methods were adopted while obtaining the spectra. In the first method the whole wave record was used with 2048 data points and a single wave spectrum was obtained (Fig. 9 to Fig. 11). In the second method, 8 consecutive sets, each of 256 points of the wave data, were considered to obtain wave spectra and all such spectra were averaged to obtain an averaged wave spectrum for the wave record (Fig. 12 to Fig. 14). The spectral amplitude of the long wave periods or low frequency waves with frequency less than 0.05Hz (or wave period greater than 20 s) were predominantly observed during the low tide and mid tide compared to high tide (Figs 9-14(a, b)) and during high tide their magnitude was comparatively less (Figs 9-14(c)). The presence of long period waves during low tides and near absence during high tides would confirm the proposition of long period wave formations due to wave breaking or wave groups in surfzone (e.g., Guza et al., 1984; Schäffer, 1993; Symonds et al., 1982; Wright et al., 1982 and others). At Miramar, the spectral amplitude of waves in lower frequency range (< 0.05 Hz) during mid tide was almost double that observed during high tide (Fig. 9), whereas at Candolim, the low frequency wave spectral amplitudes during low tide were more than twice the spectral amplitude during high tide (Fig. 10). However, at Keri, low frequency waves were persistent during all the tidal elevations, although their magnitude was declining with the increased water levels (Fig. 11).

Measured wave parameters in water depths of 13m CD off Karwar (14.82°N; 74.05°E), located 75km south of the study location are obtained from INCOIS web site (<http://www.incois.gov.in/portal/datainfo/wrb.jsp>) and are shown in Fig. 15. These wave parameters are considered as representative offshore waves for this region. Since there were no other wave measurements in the vicinity of the study area, these waves are considered as representative offshore waves. The waves were observed to be predominantly from SW direction with the significant wave heights varying between 0.6 and 1.0 m. The mean wave period was observed to vary between 4s to 9.5 s.

The wave height and mean wave period values obtained from the wave analysis for each of the record viz., significant wave height (H_s), Maximum wave height (H_{max}), 10% highest wave

height ($H_{1/10}$), the average wave height (H_{mean}) using wave by wave method, show clearly that the surfzone wave height increased with time during a flood tide (Fig. 16). However, the mean wave period decreased with time during the flood tide up to almost the mid tide and then increased during the rest of the measurement period at Keri and Miramar beaches (Fig. 17). At Candolim, the reversing trend of mean wave period increase is observed to occur much before reaching the mid tide level. The variation of mean wave period from low tide to the end of measurement period showed that Miramar, characterised by a long surfzone had the highest variation (14s to 6s) and for Candolim (6s to 9s) whereas the variation at Keri beach, highly reflective beach with a short surfzone width showed the lowest variation (13.5s to 8.5s). The maximum wave period for Miramar, Candolim and Keri ranged respectively between from 7.5s-17.5s, 9.5s-14.5s and 10.5s-19.5s. The variation of surfzone breaker index ($\gamma = H_s/\text{depth}$) with time (Fig. 18) showed a decreasing trend overall for all the three beaches. This trend is in line with the fact that the wave breaking reduces at a point as the water depth increases. The surfzone breaker index at Miramar and Keri beaches were of similar order of magnitude (0.2 to 0.3) whereas at Candolim, it was between 0.36 - 0.46, due to large breakers during the measurement period. These values are in similar order of magnitude (0.34 - 0.48) as observed by Thornton and Guza(1986), in their field measurements at Leadbetter beach, California, USA. The variation of wave height with time (Fig. 16) and variation of breaker index with time (Fig. 18) show that the increase in wave heights do not result in increased breaker index which would mean that the surfzone is unsaturated for all of these three beaches. The variation of Iribarren number with time, considering no variation in beach slope, presented in Fig. 19 showed a decreasing trend with increase of tide level for all the three locations. For Miramar these values decreased from 1.11 to 0.33 indicating initial plunging waves during low tide changing to spilling waves near high tide time. At Candolim Iribarren numbers reduced from 1.42 to 0.71 indicating the waves were predominantly plunging irrespective of tide variation of over 1m. At Keri beach the Iribarren number varied from 4.70 to 2.35 indicating predominantly surging or collapsing waves, owing to steep near shore slope. The type of breakers observed visually during the study corroborate in general with the estimated breaker type using Iribarren number.

5. Conclusions

The unsaturated surfzone wave climate at Miramar, Candolim and Keri beaches, Goa, on the central west coast of India, measured during a flood tide using a Wave and Tide gauge is presented in this paper. Such a surfzone wave data in very shallow depths is almost unavailable in this region, and therefore this paper presents valuable information related to surfzone waves and their variation with rising tide. The measured wave data is subjected to FFT analysis and wave by wave methods

and wave heights were obtained. The presence of long period waves during low tide period and mid tide period and their almost absence during high tide time once again presents a proof of the hypothesis in the literature that the wave breaking, predominant during the low tide, induces generation of long period waves. The full wave record (2048 data points) used in the FFT analysis to establish the long period waves was observed to result in better description than applying the averaging of spectra obtained from shorter wave records (256 points). Though the spectrum looks clear with the averaging method, the long wave energy is not clearly represented. The breaker index is in the range of 0.23 to 0.46, and is also observed to be reducing with increasing water levels. The surf similarity parameter indicated the variation of type of breaking as observed during the study.

6. Acknowledgements

Authors acknowledge the support of their organisation CSIR-National Institute of Oceanography, Goa. The two reviewers and the editor are greatly acknowledged for their critical reviews and in improving the manuscript significantly. This is CSIR-NIO contribution no. xxxxx.

7. References

- Anonymous, 2011. "Sbe 26 seagauge" - wave and tide recorder user manual, 104 pp.
- Apotsos, A., Raubenheimer, B., Elgar, S. and Guza, R.T., 2008. Wave-driven setup and alongshore flows observed onshore of a submarine canyon. *Journal of Geophysical Research*, 113, C07025.
- Baldock, T.E., 2006. Long wave generation by the shoaling and breaking of transient wave groups on a beach. *Proc. Royal Soc. London: Ser. A*, 462(1853-1876).
- Baldock, T.E., Hare, T.J.O. and Huntley, D.A., 2004. Long wave forcing on a barred beach. *Journal of Fluid Mechanics*, 503(321-343).
- Baldock, T.E. and Huntley, D.A., 2002. Long wave forcing by the breaking of random gravity waves on a beach. *Proceedings of the Royal Society of London: Series A*, 458: 2177-2201.
- Baldock, T.E., Huntley, D.A., Bird, P.A.D., O'Hare, T.J. and Bullock, G.N., 2000. Breakpoint generated surf beat induced by bichromatic wave groups. *Coastal Engineering*, 39: 213-242.
- Basco, D.R., 1983. Surfzone currents. *Coastal Engineering*, 7(4): 331-355.
- Bird, E.C.F., 1985. *Coastline changes*. Wiley & Sons, New York, 219 pp.
- Chandramohan, P., Sanil Kumar, V., Nayak, B.U. and Pathak, K.C., 1993. Variation of longshore current and sediment transport along the south maharashtra coast, west coast of india. *Indian Journal of Marine Sciences*, 22: 115-118.

- Dally, W.R., Dean, R.G. and Dalrymple, R.A., 1985. Wave height variation across beaches of arbitrary profile. *Journal of Geophysical Research*, 90(C14): 11917-11928.
- Dean, R.G. and Dalrymple, R.A., 2010. *Water wave mechanics for engineers and scientists. Advanced series on ocean engineering, 2.* World scientific publications.
- Dong, G. et al., 2009. Experimental study of long wave generation on sloping bottoms. *Coastal Engineering*, 56(1): 82-89.
- Elfrink, B. and Baldock, T.E., 2002. Hydrodynamics and sediment transport in swash zone: A review. *Coastal Engineering*, 45: 149-167.
- Fredsøe, J. and Deigaard, R., 1992. *Mechanics of coastal sediment transport. Advanced series on ocean engineering - volume 3.* World Scientific, 369 pp.
- Guza, R.T., Thornton, E.B. and Holman, R.A., 1984. Swash on steep and shallow beaches. *Proceedings of the 19th International Conference on Coastal Engineering*: 708-723.
- Hamm, L., Madsen, P.A. and Peregrine, D.H., 1993. Wave transformation in the nearshore zone: A review. *Coastal Engineering*, 21(1-3): 5-39.
- Janssen, T.T., Battjes, J.A. and Van Dongeren, A.R., 2003. Observations of long waves induced by short wave groups. *Journal of Geophysical Research*, 108: 3252-3264.
- Kuik, A.J., van Vledder, G.P. and Holthuijsen, L.H., 1988. A method for the routine analysis of pitch-and-roll buoy wave data. *Journal of Physical Oceanography*, 18(7): 1020-1034.
- Longuet-Higgins, M.S. and Stewart, R.W., 1962. Radiation stresses and mass transport in gravity waves, with application to 'surf beats'. *Journal of Fluid Mechanics*, 13(4): 481-504.
- Madsen, P.A., Sørensen, O.R. and Schäffer, H.A., 1997. Surf zone dynamics simulated by a boussinesq type model. Part i. Model description and cross-shore motion of regular waves. *Coastal Engineering*, 32(4): 255-287.
- Munk, W.H., 1949. Surf beats. *Transactions of American Geophysical Union*, 30(6): 849-854.
- Nielsen, P., 2009. *Coastal and estuarine processes. Advanced series on ocean engineering.* World Scientific, New York, NJ (USA), 343 pp.
- Omran, E.F., Essam, A.D. and Ahmed, A.E., 2010. Wave climate and nearshore processes on the mediterranean coast of egypt. *J. Coast. Res.*, 26: 103-112.
- Power, H.E., Hughes, M.G., Aagaard, T. and Baldock, T.E., 2010. Nearshore wave height variation in unsaturated surf. *J. Geophys. Res.*, 115(C08030).
- Reginald, A.B. and Richard, W.S., 1988. Suspended sediment transport in the surf zone: Response to cross-shore infragravity motion. *Marine Geology*, 80(1-2): 61-79.
- Rogers, A.L. and Ravens, T.M., 2008. Measurement of longshore sediment transport rates in the surf zone on galveston island, texas. *Journal of Coastal Research*, 23: 62-73.

- Sanil Kumar, V., M., A.N., Chandramohan, P. and Naik, G.N., 2003. Longshore sediment transport rate-measurement and estimation, central west coast of india. *Coastal Engineering*, 48(2): 95-109.
- Sanil Kumar, V., Pathak, K.C., Pednekar, P., Raju, N.S.N. and Gowthamn, R., 2004. Coastal processes along the indian coastline. *Current Science*, 91: 530-536.
- Schäffer, H.A., 1993. Infragravity waves induced by short wave groups. *Journal of Fluid Mechanics*, 247: 551-588.
- Seelam, J.K. et al., 2014. Post monsoon equilibrium beach profiles and longshore sediment transport rates at candolim, miramar and keri beaches of goa, india. *Current Science*, 106(3): 408-416.
- Sørensen, O.R., Schäffer, H.A. and Madsen, P.A., 1998. Surf zone dynamics simulated by a boussinesq type model. Iii. Wave-induced horizontal nearshore circulations. *Coastal Engineering*, 33(2-3): 155-176.
- Symonds, G., Huntley, D.A. and Bowen, A.J., 1982. Two dimensional surf beat: Long wave generation by a time-varying breakpoint. *Journal of Geophysical Research*, 87(492-498).
- Thornton, E.B. and Guza, R.T., 1986. Surf zone long shore currents and random waves: Field data and models. *Journal of Physical Oceanography*, 16: 1165-1178.
- Tucker, M.J., 1950. Surf beats: Sea waves of 1 to 5 minute period. *Proc. Royal Soc. London: Ser. A*, 202: 565-573.
- Wright, L.D., Guza, R.T. and Short, A.D., 1982. Dynamics of a high energy dissipative surf zone. *Marine Geology*, 45: 41-62.

Table 1. Geographical positions of the three beaches

Sl. No	Station	Latitude	Longitude	Date of wave measurements
1	Miramar	15°28'57" N	73°48'27" E	18 January 2012
2	Candolim	15°30'38" N	73°45'53" E	19 January 2012
3	Keri	15°43'05" N	73°41'25" E	17 January 2012

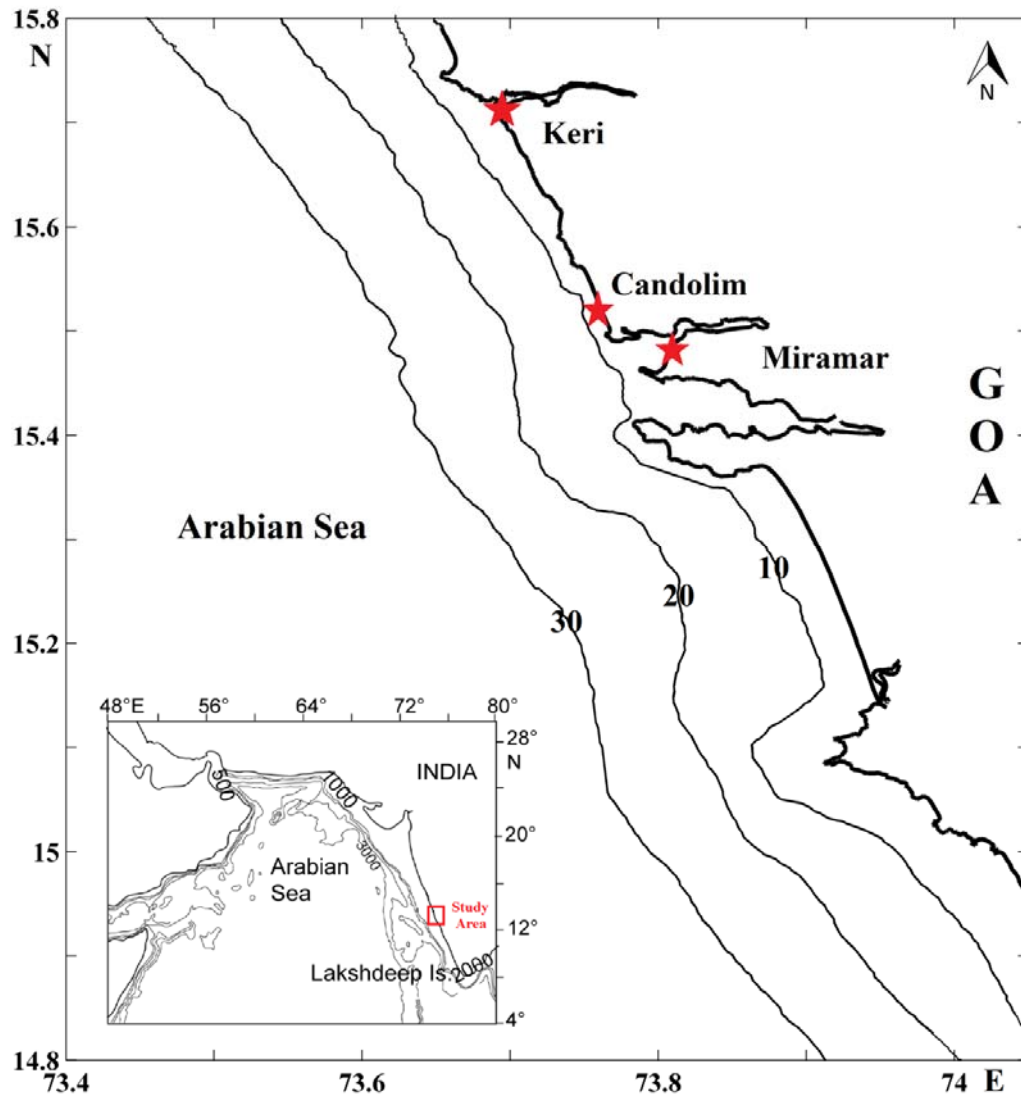
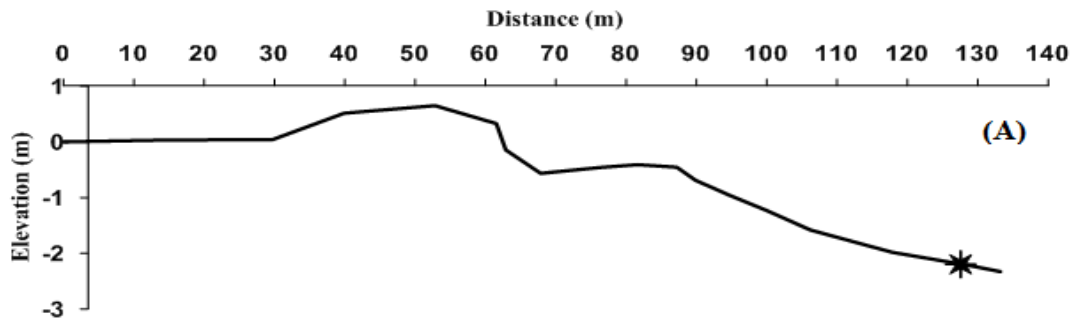


Fig.1. Location map of the study region



(b)

Fig.2. (a) Location of WTG and (b) cross section profile at Miramar beach

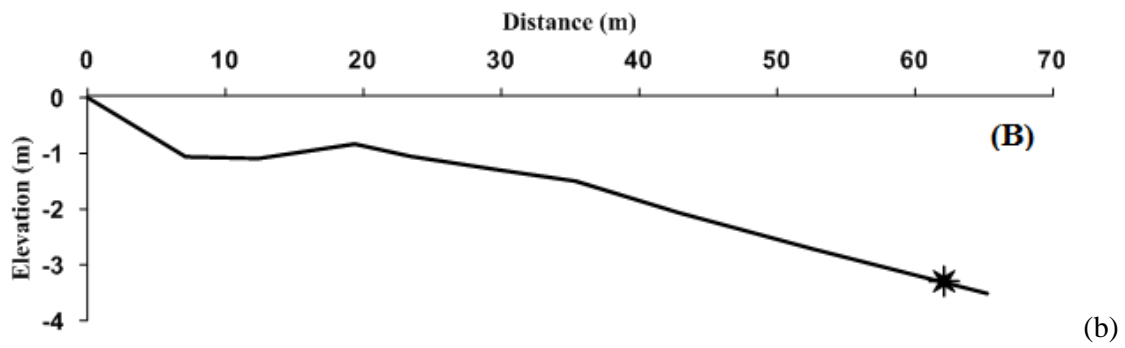


Fig.3. (a) Location of WTG and (b) cross section profile at Candolim beach

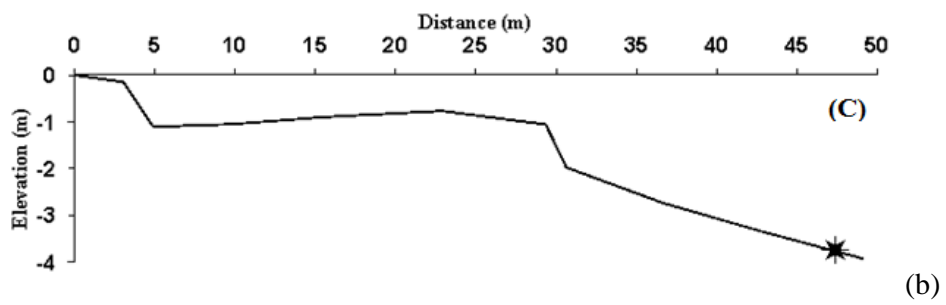


Fig.4. (a) Location of WTG and (b) cross section profile at Keri beach

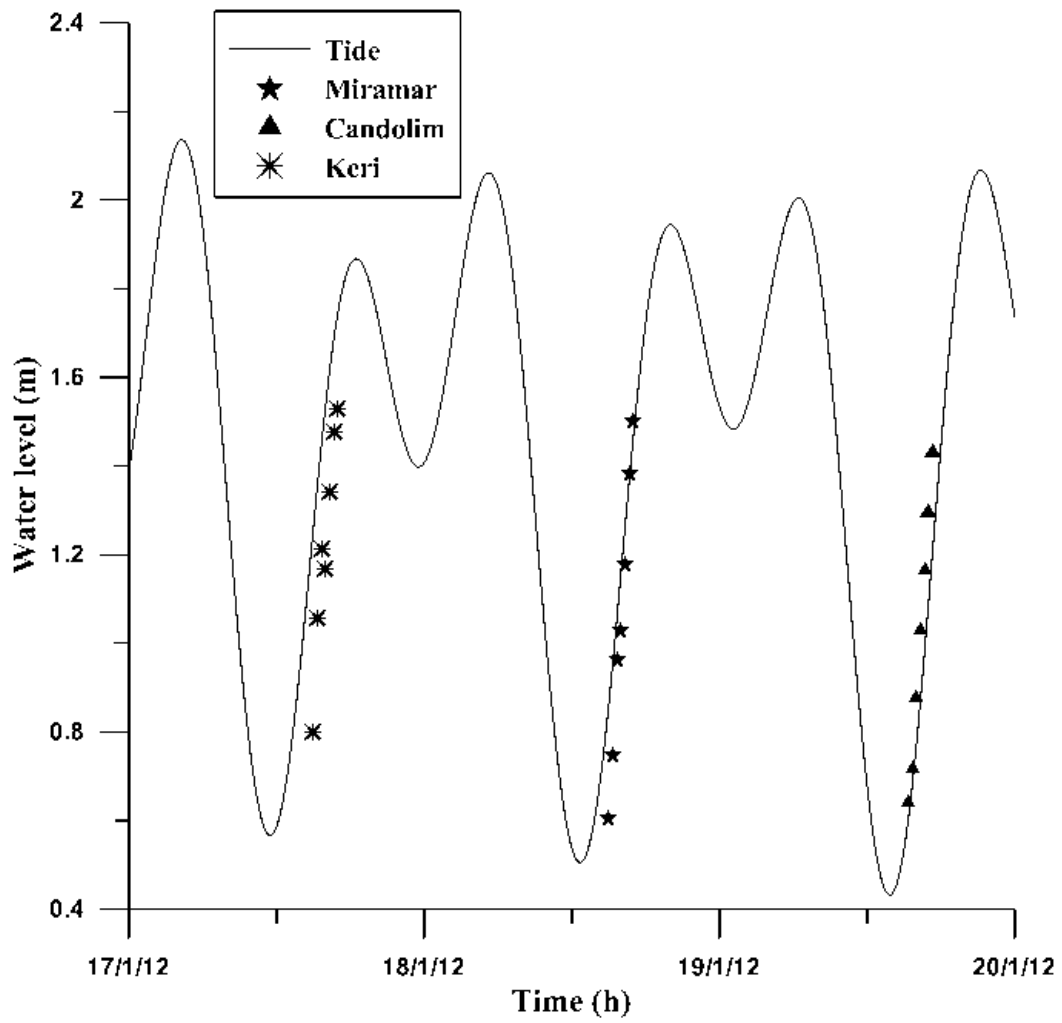


Fig.5. Variation of predicted tide (solid line) and the measured water levels (symbols).

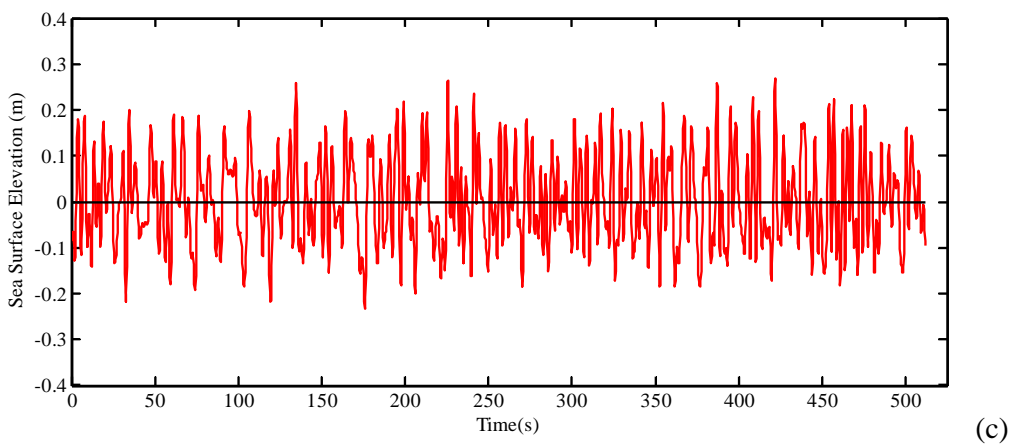
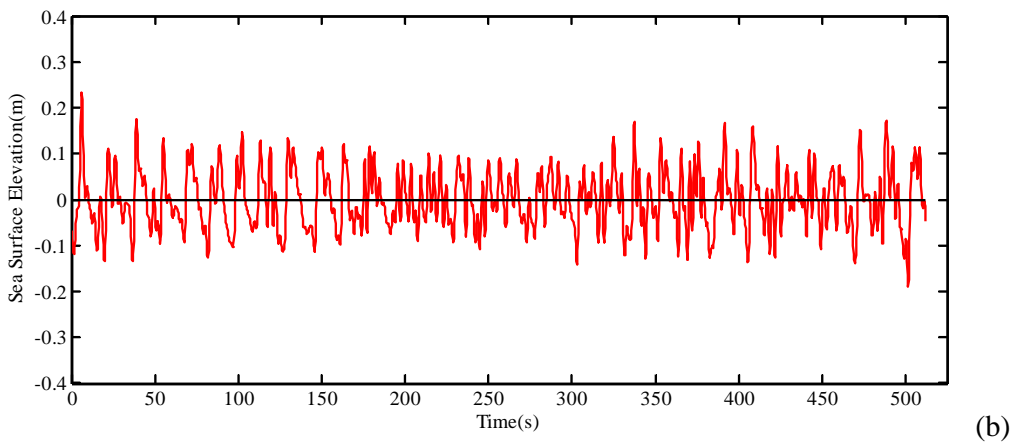
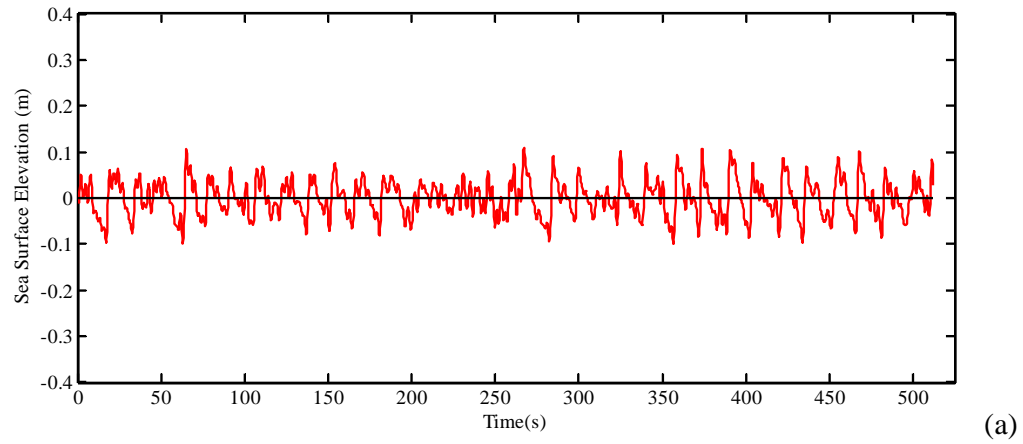


Fig.6. Filtered wave data plots for Miramar during (a) low tide (b) mid tide and (c) High tide level

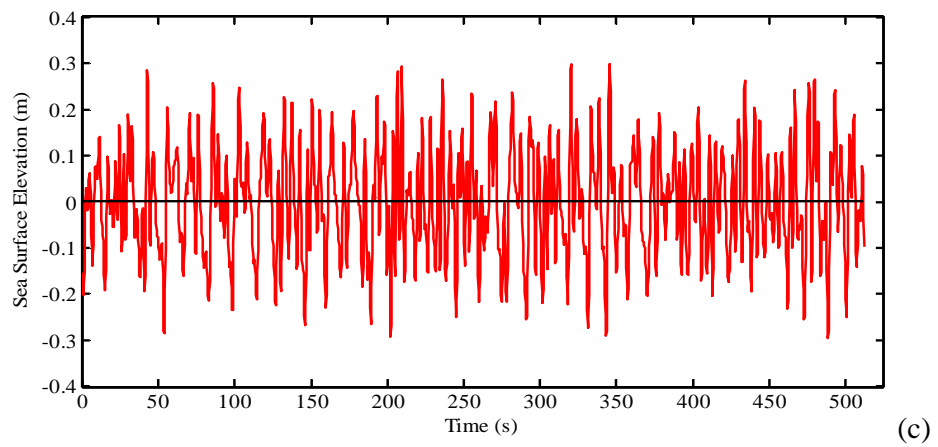
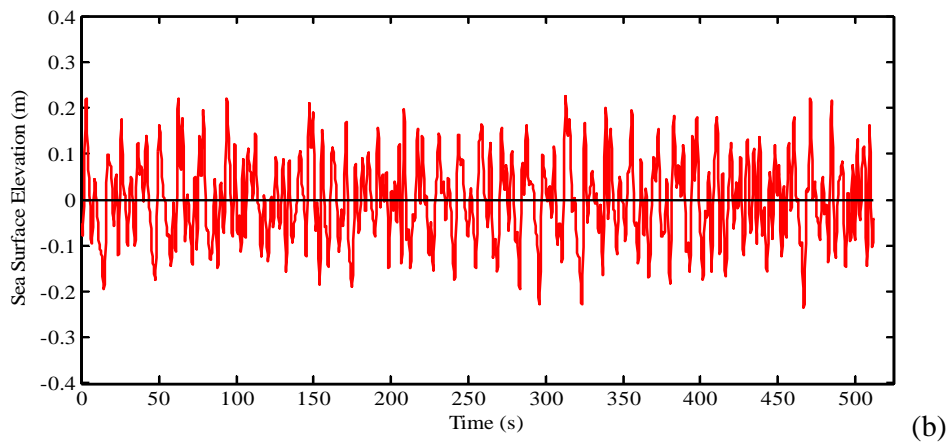
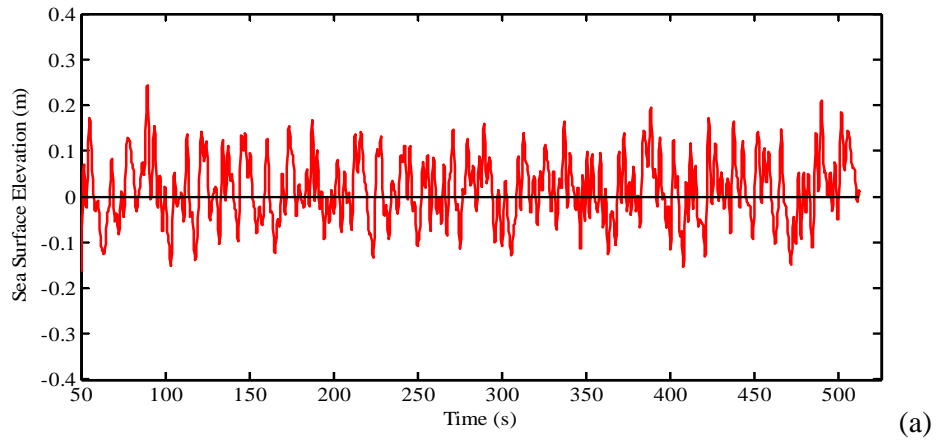


Fig.7. Filtered wave data plots for Candolim during (a) low tide (b) mid tide and (c) High tide level

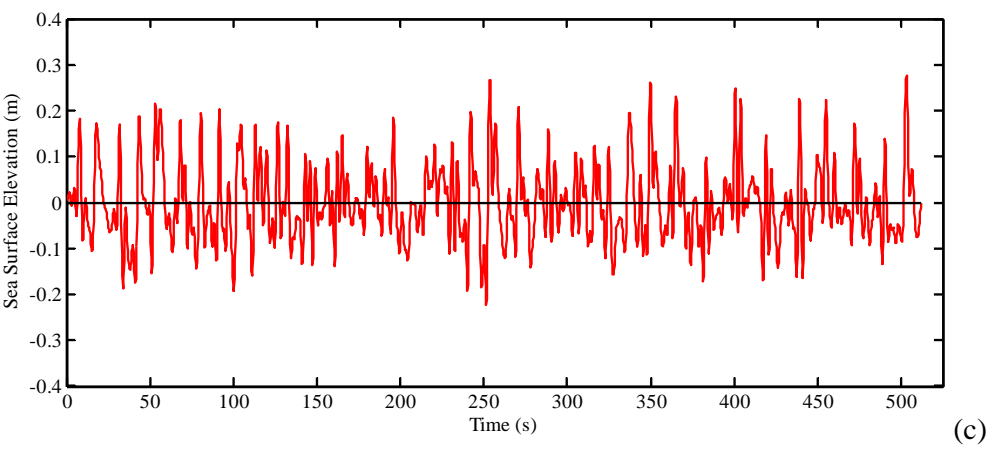
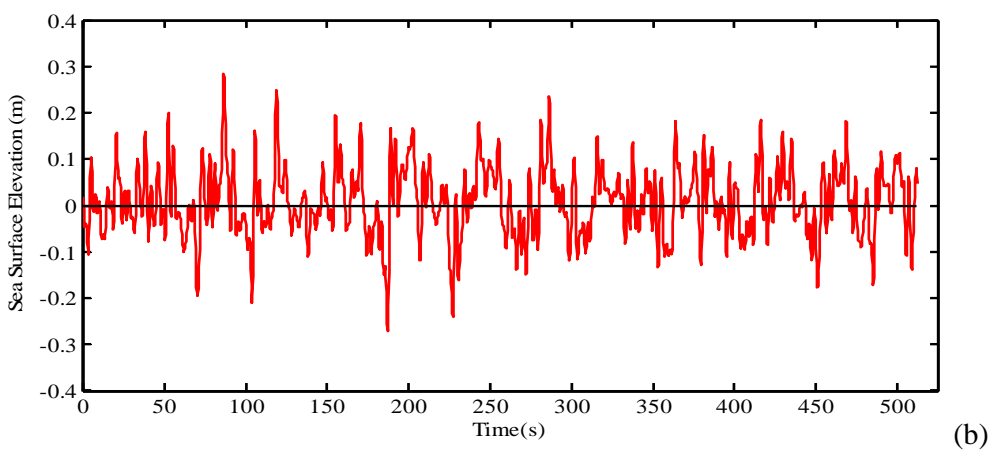
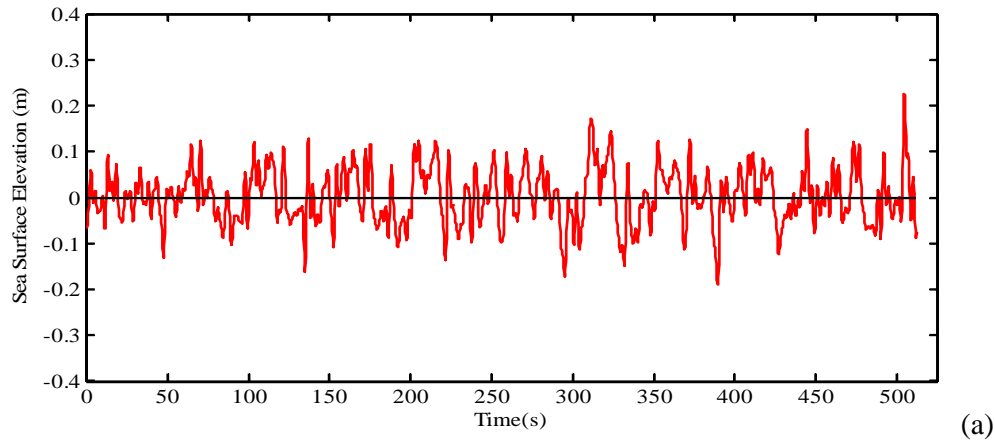


Fig.8. Filtered wave data plots for Keri during (a) low tide (b) mid tide and (c) High tide level

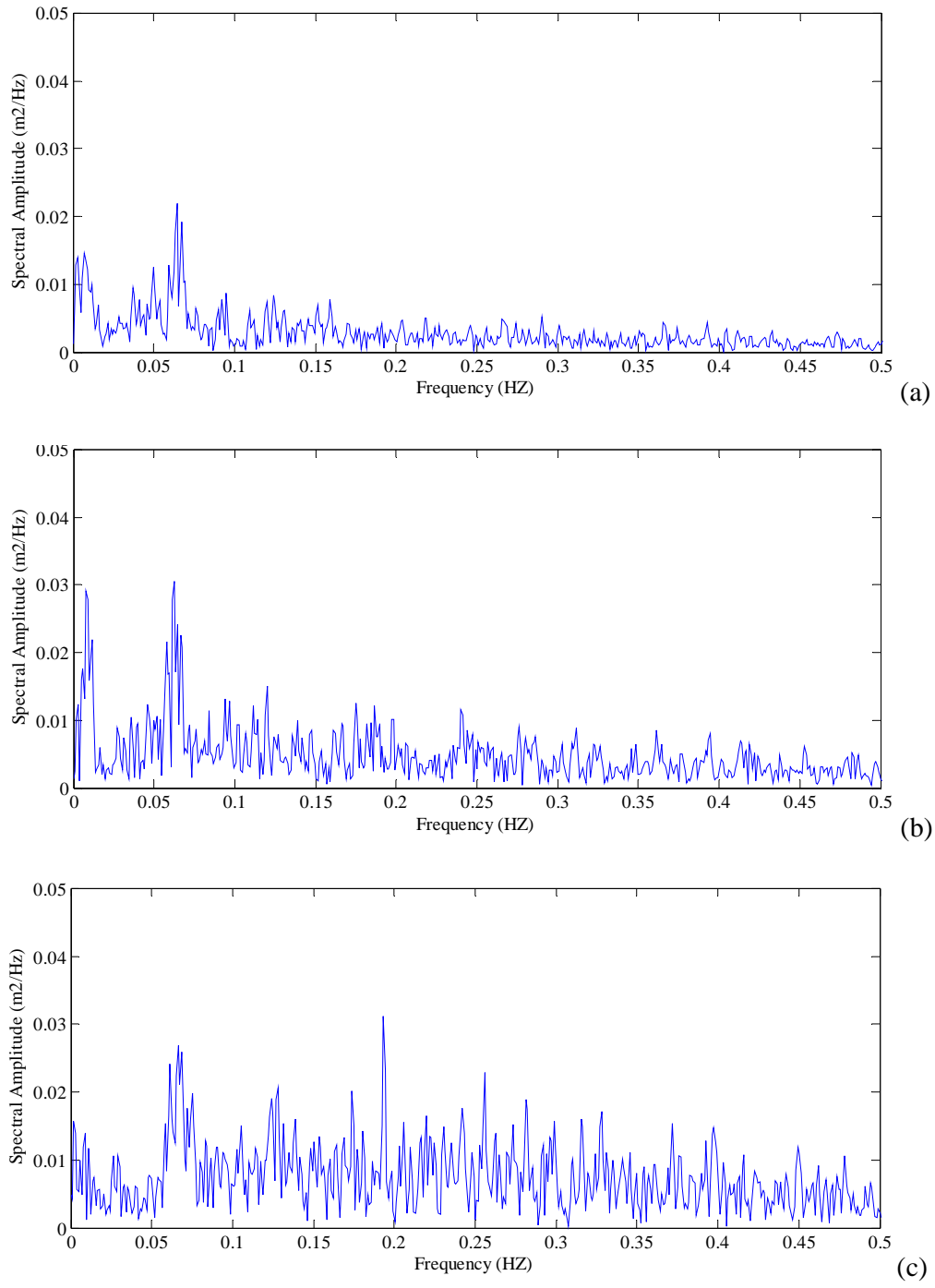


Fig.9. Wave spectra at Miramar during (a) low tide (b) mid tide and (c) high tide

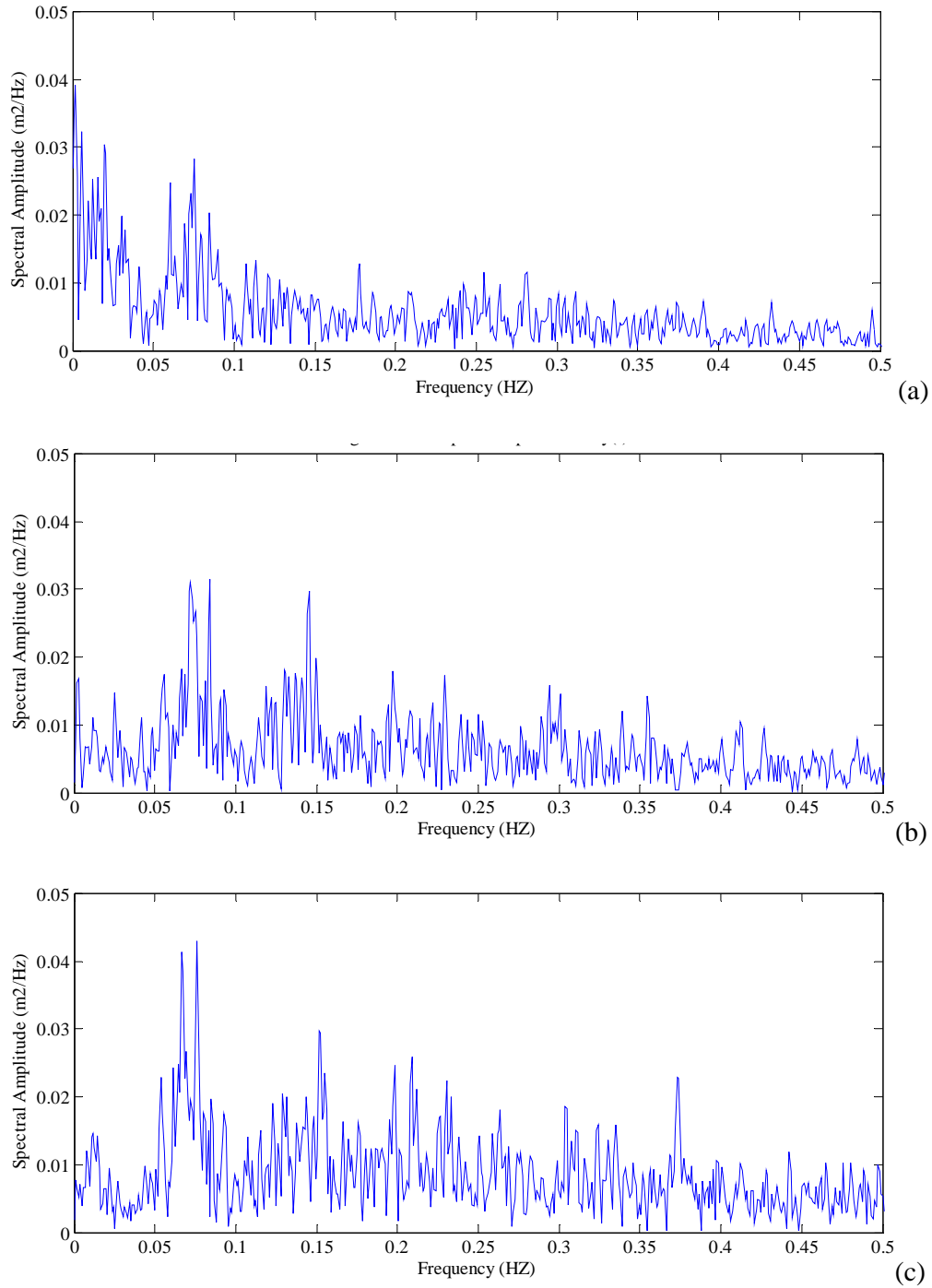


Fig.10. Wave spectra at Candolim beach during (a) low tide (b) mid tide and (c) high tide.

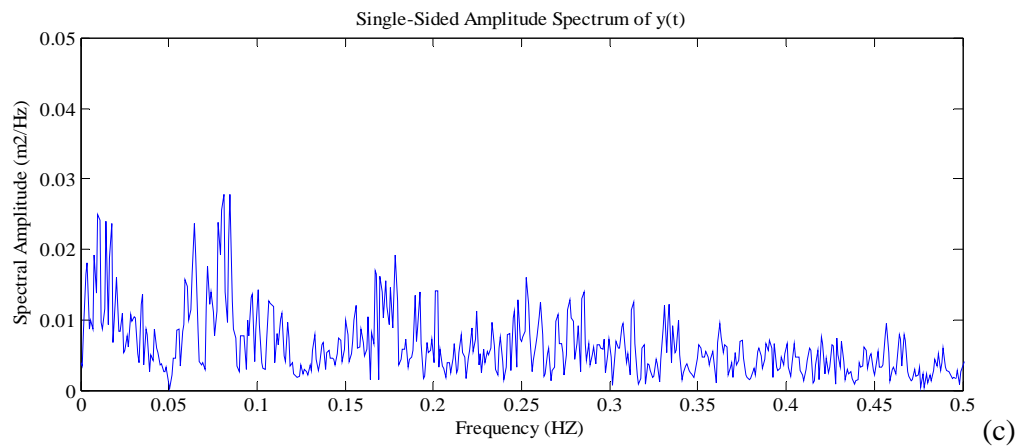
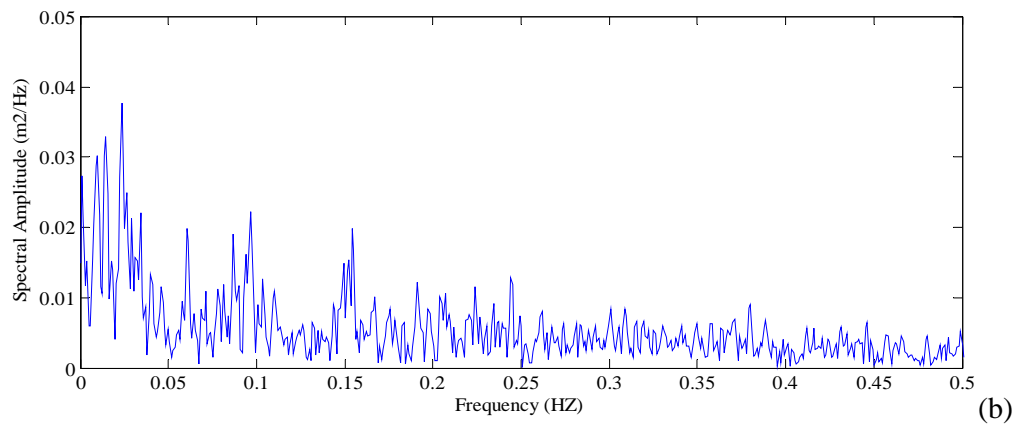
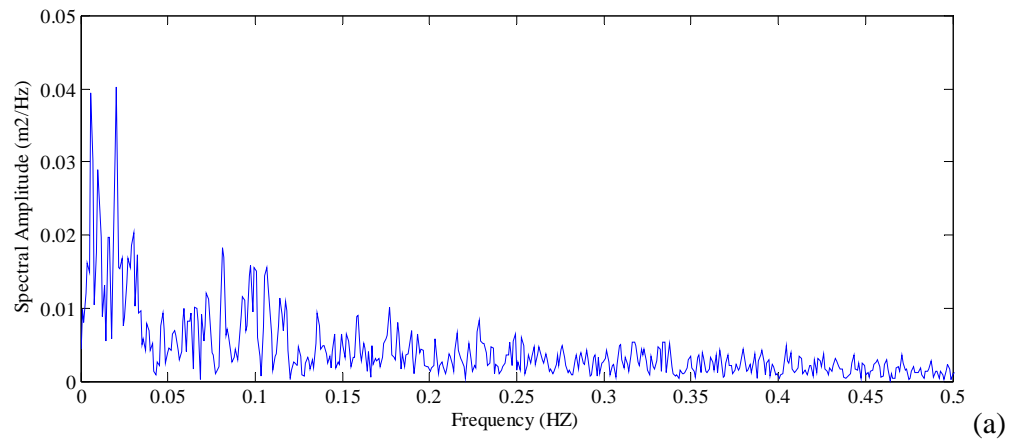


Fig.11. Wave spectra at Keri beach during (a) low tide (b) mid tide and (c) high tide.

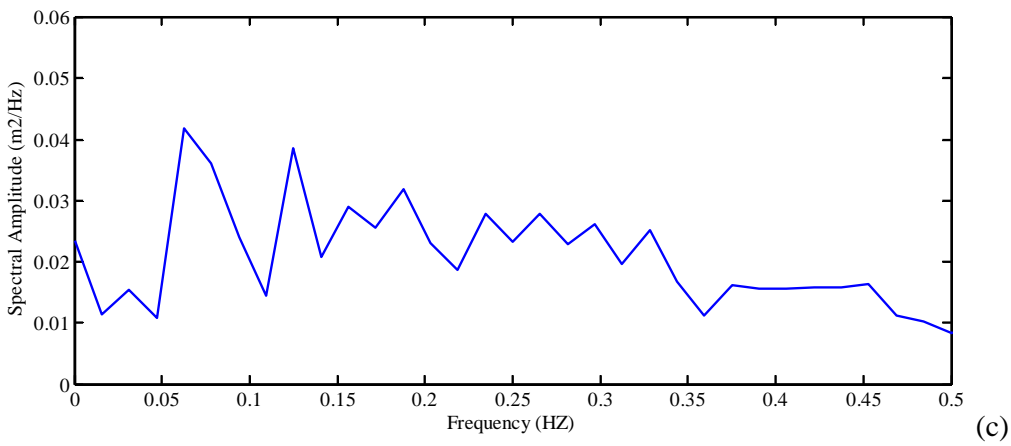
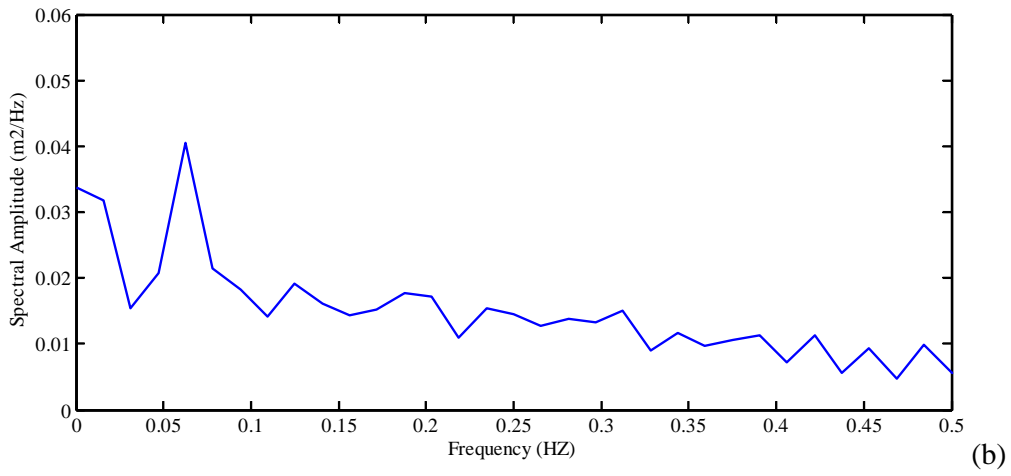
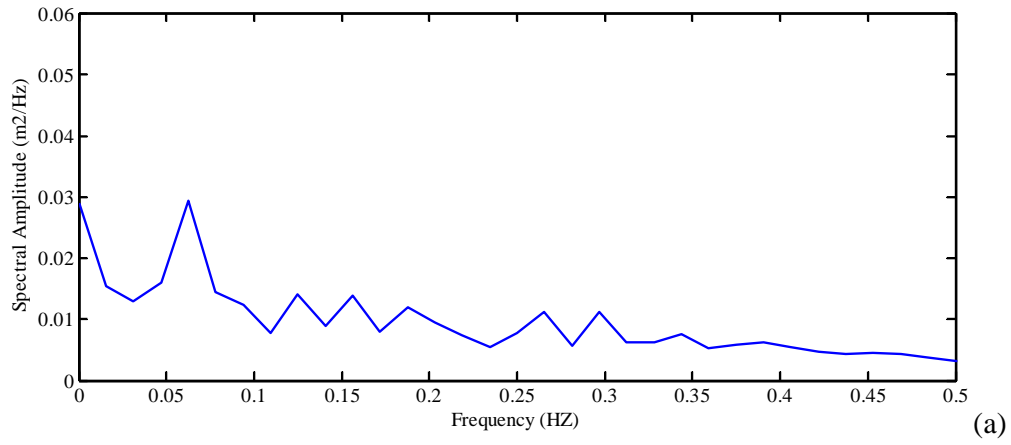


Fig.12. Averaged wave spectra at Miramar during (a) low tide (b) mid tide and (c) high tide.

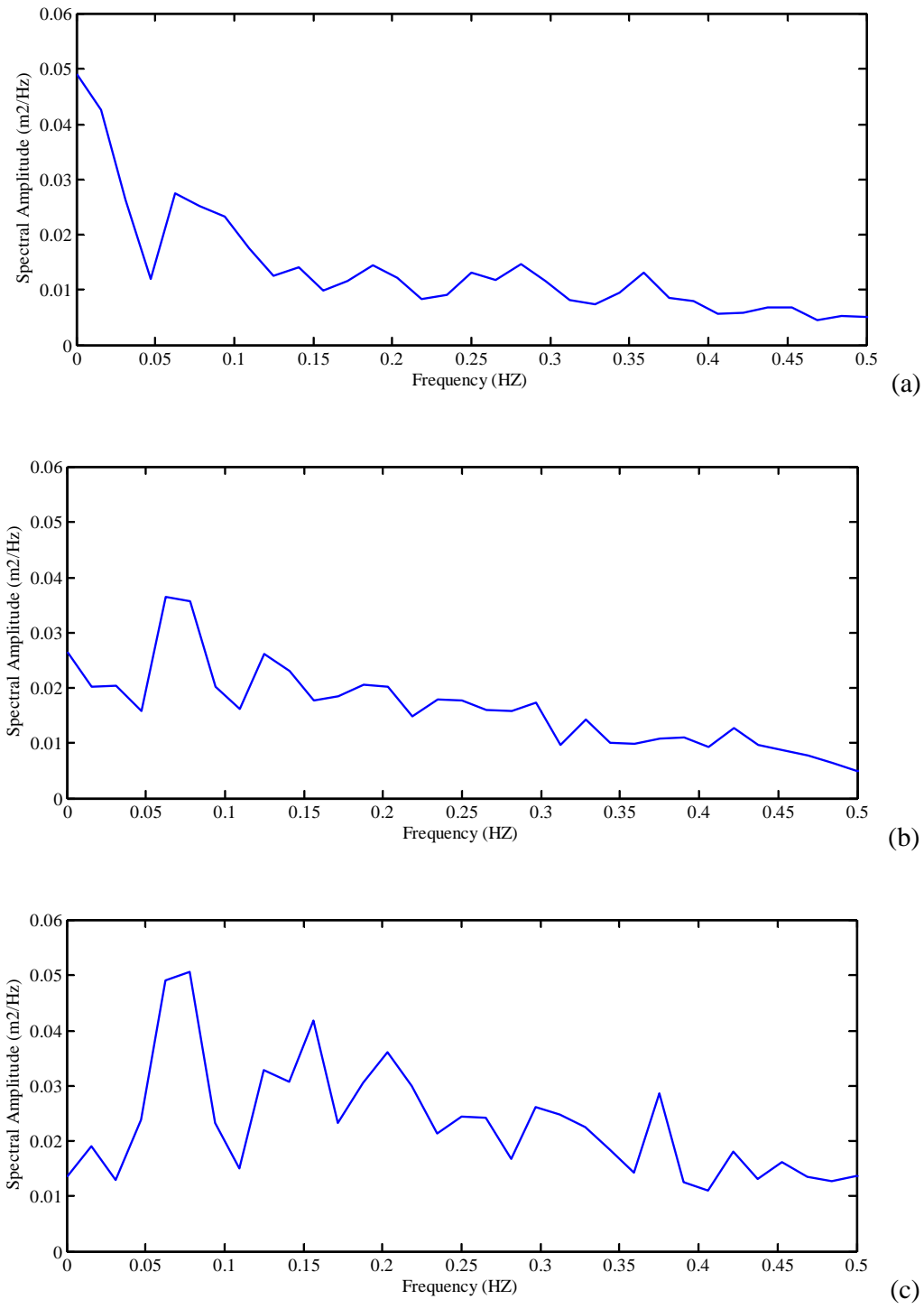


Fig.13. Averaged wave spectra at Candolim beach during (a) low tide (b) mid tide and (c) high tide.

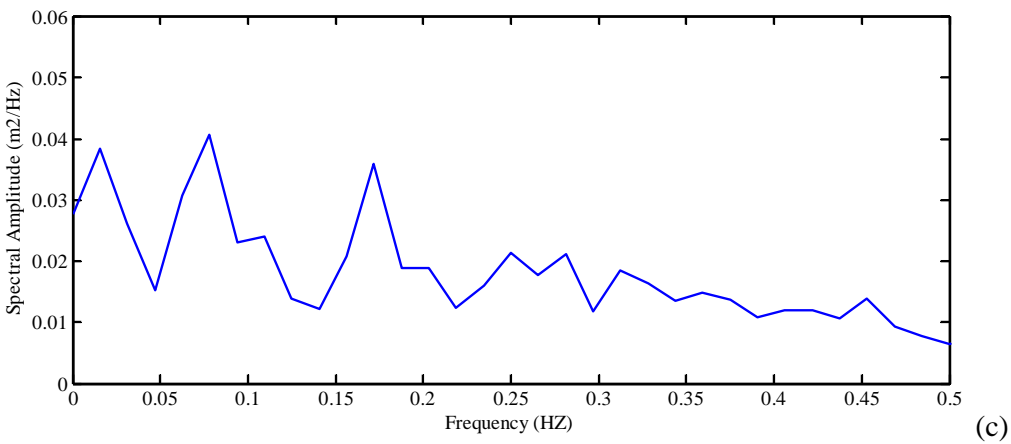
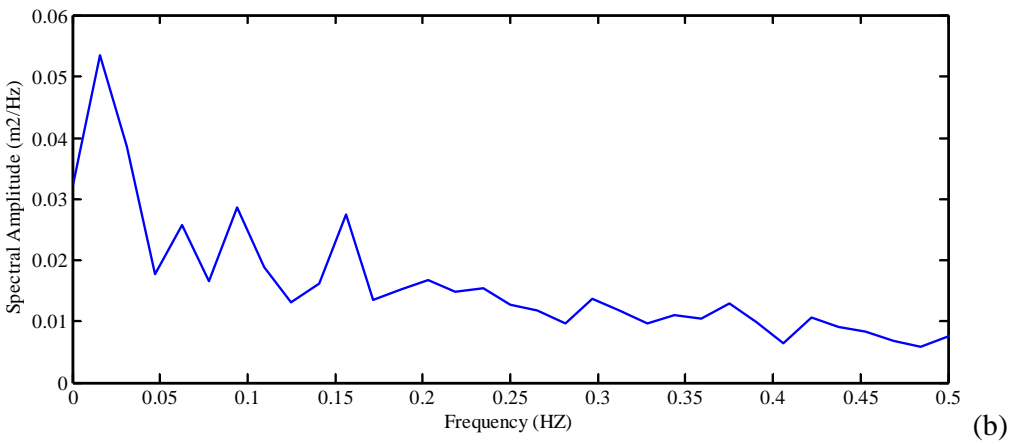
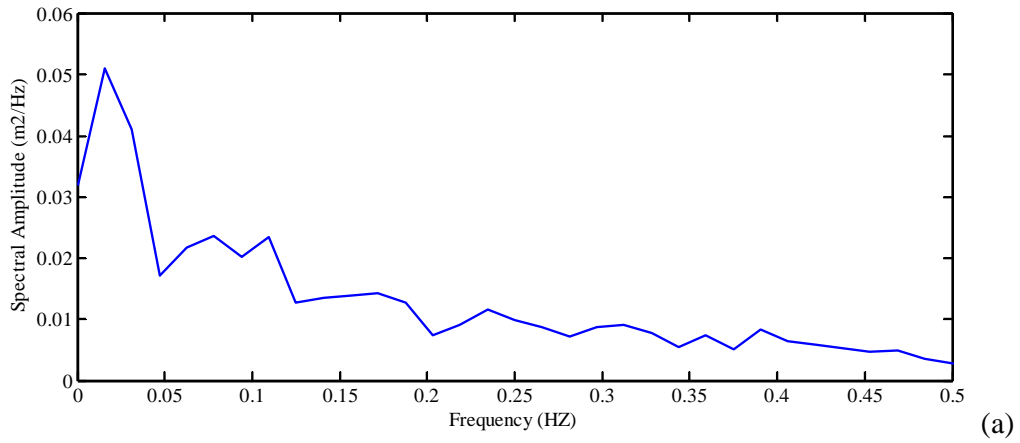


Fig.14. Averaged wave spectra at Keri beach during (a) low tide (b) mid tide and (c) high tide.

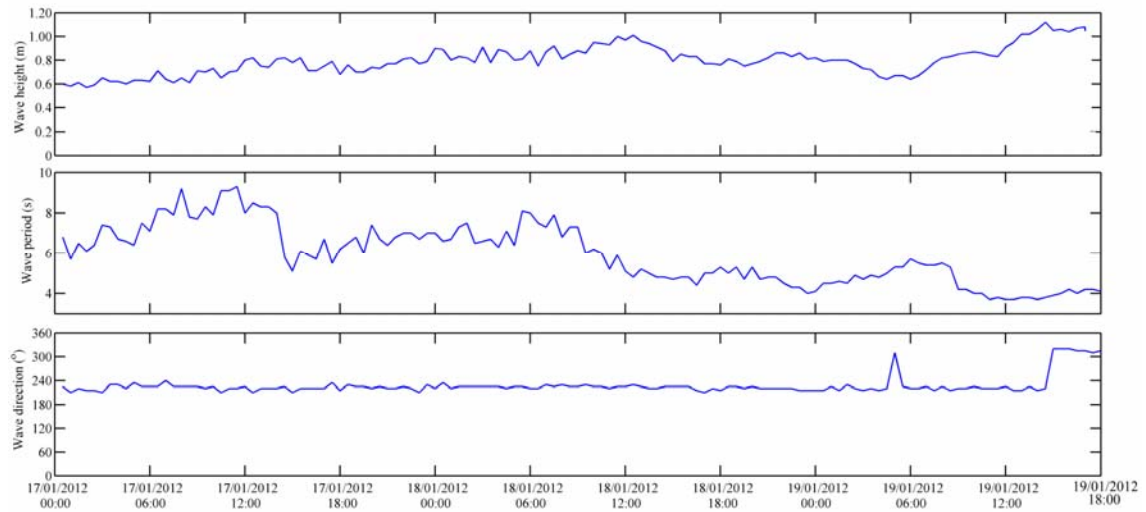


Fig.15. Variation of wave height, wave period and wave direction off Karwar.

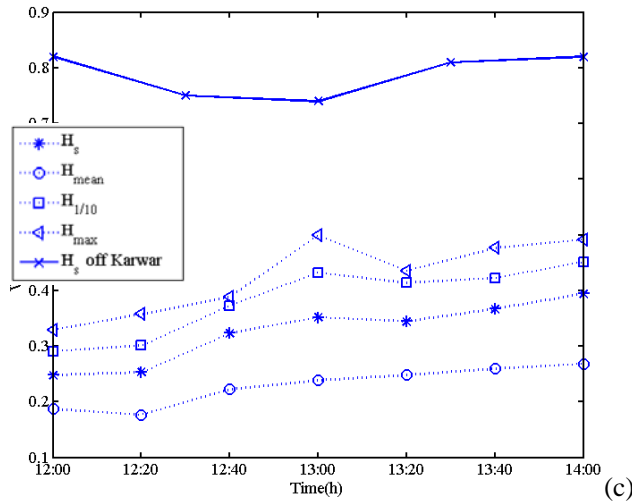
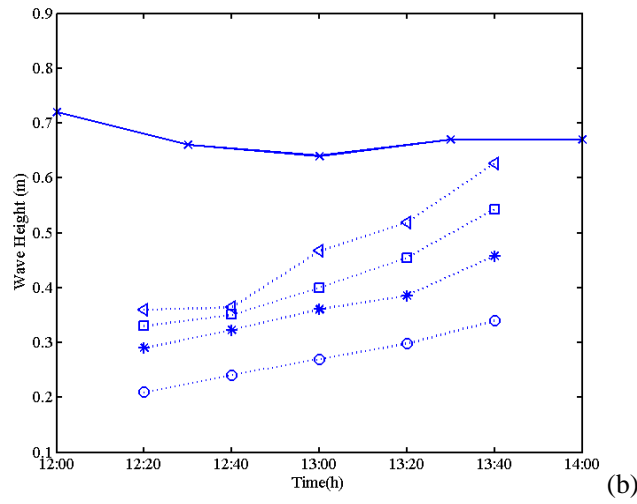
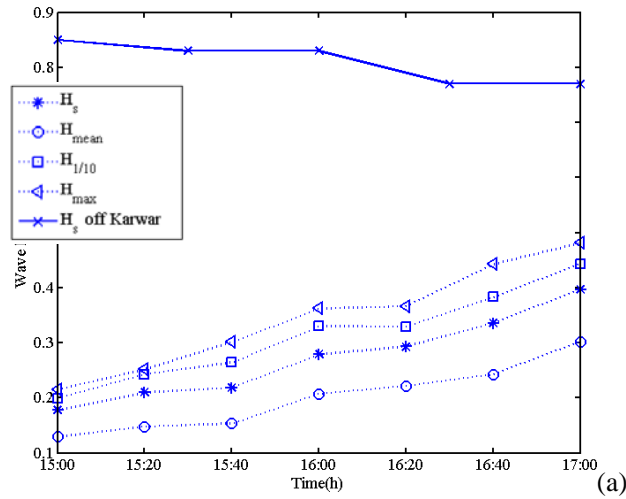


Fig.16. Variation of wave heights with time for (a) Miramar, (b) Candolim and (c) Keri beaches. Solid line with x represent H_s off Karwar, stars represent H_s , circles- H_{mean} , squares- $H_{1/10}$, triangle- H_{max}

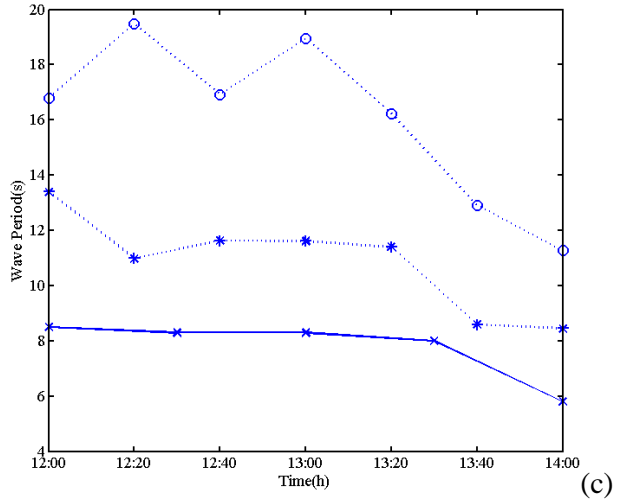
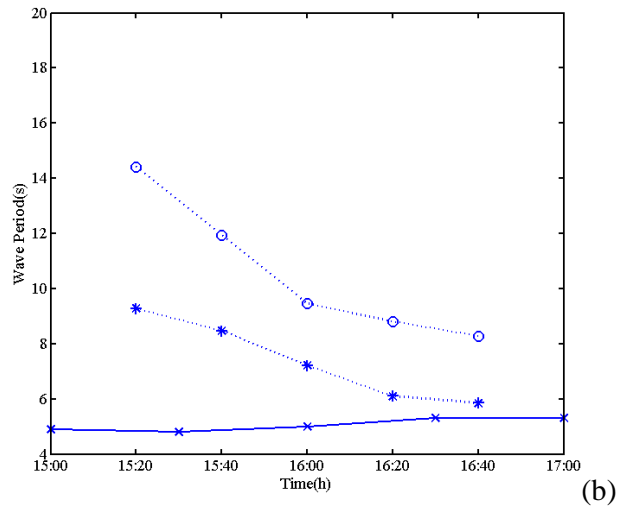
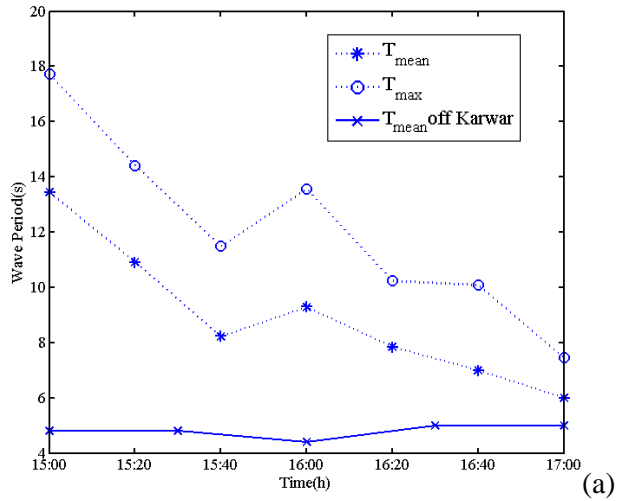


Fig.17. The mean wave period (*) and maximum period (o) for (a) Miramar, (b) Candolim and (c) Keri beaches. Solid line with x represents T_{mean} off Karwar, circles represent T_{max} , stars represent T_{mean}

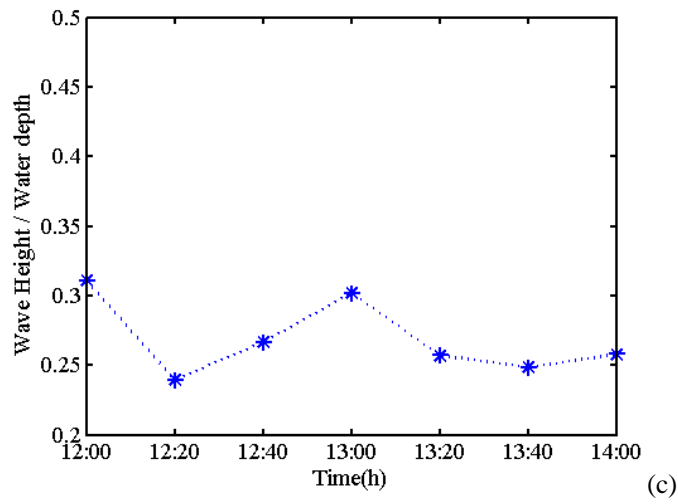
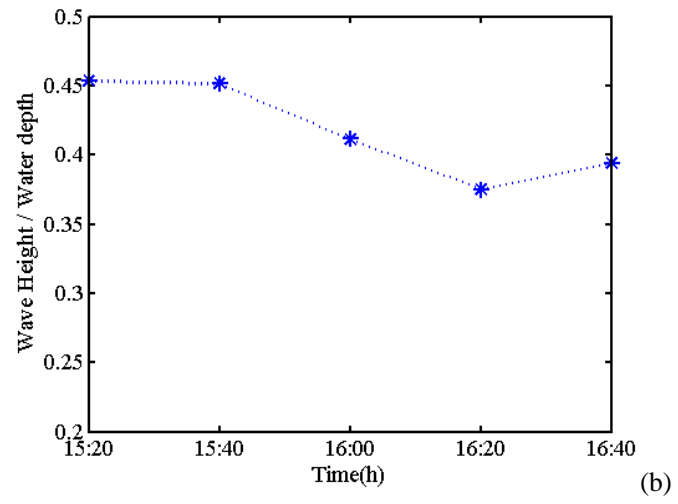
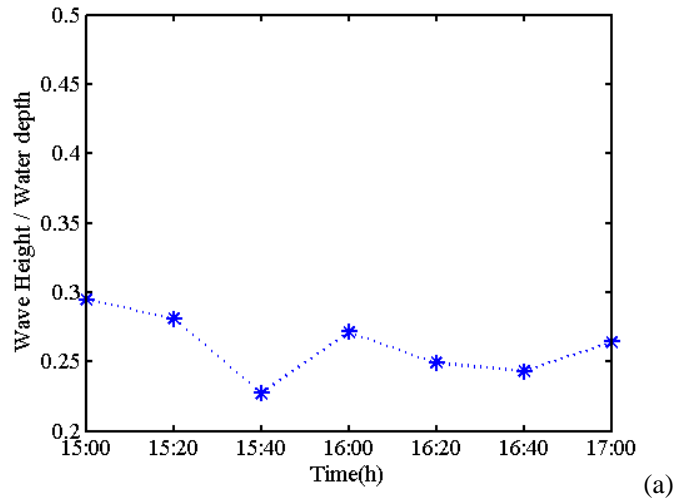


Fig.18. Variation of breaker index γ with time for (a) Miramar (b) Candolim and (c) Keri beaches

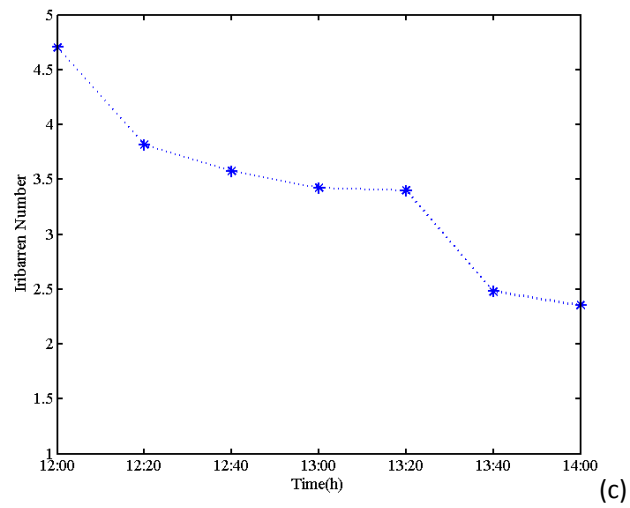
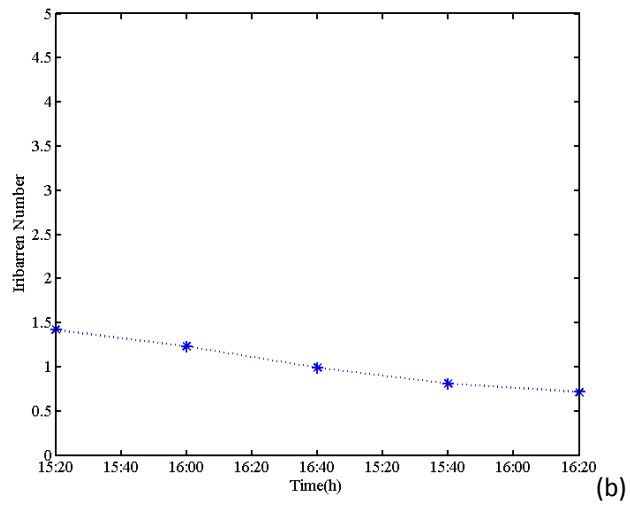
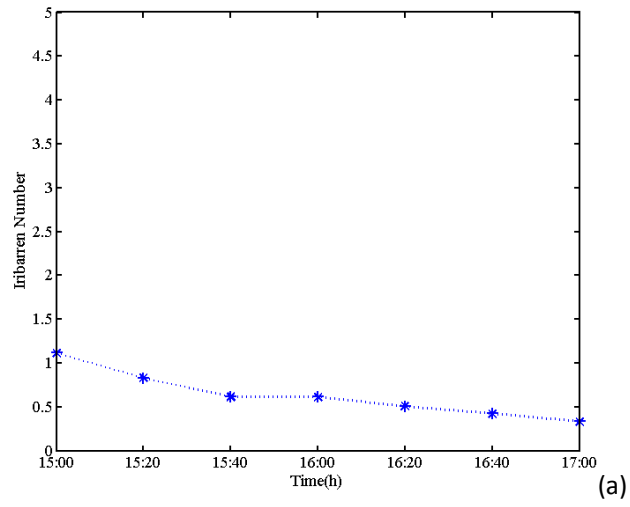


Fig.19. Variation of Iribarren Number with time for (a) Miramar (b) Candolim and (c) Keri beaches